International Journal of Minerals, Metallurgy and Materials
Volume 29, Number 10, October 2022, Page 1932
https://doi.org/10.1007/s12613-022-2467-7

Invited Review

Hematite reduction by hydrogen plasma: Where are we now?

Kali Charan Sabat✉

Department of Materials and Metallurgical Engineering, Maulana Azad National Institute of Technology, Bhopal, 462003, Madhya Pradesh, India
(Received: 24 January 2022; revised: 6 March 2022; accepted: 7 March 2022)

Abstract: Currently, iron is extracted from ores such as hematite by carbothermic reduction. The extraction process includes several unit steps/processes that require large-scale equipment and significant financial investments. Additionally, the extraction process produces a substantial amount of harmful carbon dioxide (CO_2). Alternative to carbothermic reduction is the reduction by hydrogen plasma (HP). HP is mainly composed of exciting species that facilitate hematite reduction by providing thermodynamic and kinetic advantages, even at low temperatures. In addition to these advantages, hematite reduction by HP produces water, which is environmentally beneficial. This report reviews the theory and practice of hematite reduction by HP. Also, the present state of the art in solid-state and liquid-state hematite reduction by HP has been examined. The in-flight hematite reduction by HP has been identified as a potentially promising alternative to carbothermic reduction. However, the in-flight reduction is still plagued with problems such as excessively high temperatures in thermal HP and considerable vacuum costs in non-thermal HP. These problems can be overcome by using non-thermal atmospheric HP that deviates significantly from local thermodynamic equilibrium.

Keywords: hematite; iron ore; hematite reduction; iron production; hydrogen plasma; non-thermal plasma; thermodynamics; kinetics

1. Introduction

Iron (Fe) is typically produced by carbothermic reduction of medium/high-grade iron ores, including hematite. Carbothermic reduction makes use of carbon derived from coke, made from coking coal. The future availability of both these raw materials is limited because of the depletion throughout the world. Furthermore, the production process flow sheet of iron covers numerous steps, e.g., coke-making, palletization, sintering, etc. Each step is problematic, incurring significant expenses and facing tougher environmental regulations due to the emission of carbon dioxide (CO_2). In general, 1.8 t of CO_2 is discharged into the atmosphere for every ton of steel produced [1]. At present, the world steel output is 1878 million tons (MT) [2], which produces an estimated 3380 MT of CO_2 per year. This massive amount of CO_2 emitted worldwide is responsible for the greenhouse effect, pushing the globe into a risky zone for survival, with severe environmental implications of natural disasters. These natural calamities include destruction of ecosystems, loss of biodiversity, development of heatwaves, shrinking of the glaciers, increasing sea levels, massive economic losses, and so on [1]. Due to these losses and severe environmental requirements, there have been enormous efforts by steel manufacturers globally to decrease/eliminate CO_2 emissions. However, the conventional unit steps/processes of ironmaking have almost matured because of research and development (R&D) over a long period. As a result, further reductions of CO_2 emissions from the existing technologies are not conceivable [3].

2. Hydrogen gas—The alternative reductant

Because of the above-cited problems, significant R&D activities are going on worldwide in search of breakthrough technologies involving low-carbon or eliminating carbon (C). In this regard, more than one billion US dollars have already been invested [1,4]. Based on the research findings to date, hydrogen (H_2) has been identified as the best candidate to replace carbon because of its thermodynamic and kinetic advantages [1,4–6].

In addition to the thermodynamic and kinetic advantages, the consumption of H_2 is also low in comparison to C. The theoretical mass balance of reductants and products (in tons) to produce 112 t of Fe from hematite shows that 112 t of Fe production require 36 t of C, resulting in 84 t of carbon monoxide (CO). Similarly, to produce 112 t of Fe, 18 t of C are required, resulting in 66 t of CO_2. In these processes, massive amounts of CO and CO_2 are produced. Coking coal provides the massive amount of C required for these reduction processes. Coke production from coking coal is not environmentally benign, and coking coal is in short supply. Furthermore, the massive amounts of CO and CO_2 created by these processes pollute the atmosphere and contribute to the greenhouse effect. In contrast, 112 t of Fe require just 6 t of H_2 when H_2 is used as a reductant, and it produces 54 t of water, which is safe for the environment.

✉ Corresponding author: Kali Charan Sabat E-mail: kcsabat@gmail.com

When it comes to availability, coking coal of acceptable quality is becoming scarcer day by day, but H_2 is widely available in nature. For example, H_2 is produced from H_2O through H_2O splitting, and H_2O is abundant in nature. H_2 is currently manufactured in a variety of ways, including methane reforming and electrolysis of H_2O. H_2 production using solar energy is undergoing substantial study and development, such as electrolyzing H_2O by employing the necessary electrons produced by solar cells or splitting H_2O using sunlight on a semiconductor immersed in H_2O [7−8]. Also, there have been substantial efforts to use renewable energy and nuclear energy to produce H_2 economically.

Apart from the lower consumption in terms of theoretical requirement of H_2 per ton of Fe and the availability of H_2 in plentiful H_2O, H_2 has several other technical advantages: (1) The product gases of the reduction are environmental friendly mixtures of H_2O and H_2, in contrast to the detrimental mixture of CO and CO_2 produced when C is used as the reductant. (2) The kinetics of reduction is faster than the kinetics of reduction using C. (3) It avoids C content in the produced Fe, whereas C containing Fe is made when C is the reductant. (4) It avoids polluting and expensive metallurgical coke, thus avoiding CO and CO_2. (5) It decreases the energy of Fe production and CO_2 emission by 57 and 96 percent, respectively, compared to using C. The elimination of coke-making, sintering, pelletization, and other unit steps/processes, accounts for most of these benefits [9].

3. Brief Introduction to hydrogen plasma (HP)

In our daily lives, we come across four states of matter: solid, liquid, gas, and plasma. Among these, plasma constitutes 99.9% of the universe [10]. Plasmas are also employed in our daily life in some way —for example, fluorescent lights, television, industrial processes, etc. Plasma is nothing more than an energized gas. The gas excitation comes from the energy transfer to gas molecules (in this case, H_2) by direct current (DC), alternating current (AC), or an electromagnetic wave (EM) such as radiofrequency. induction, microwave, etc. Interestingly, H_2 molecules have some polarity associated with them. When the polarity of H_2 interacts with high-energy electrons associated with DC, AC, or EM, H_2 absorbs the energy by rotation, vibration, dissociation, ionization, etc. For the first rotational level, first vibrational level, dissociation, and ionization, the absorbed energy needed are 0.015, 0.516, 4.52, and 13.6 eV, respectively [11]. Furthermore, the H_2 molecules collide with one another to transmit energy. Therefore, depending on the collisions, plasmas can be of three types: (1) thermal or hot plasma, (2) non-thermal or cold plasma, and (3) mixed plasma, as shown in Fig. 1.

3.1. Thermal or hot plasma

Thermal plasma is simply an energized gas in which a large number of molecules/atoms have been ionized. They occur when H_2 molecules at considerable pressure collide with the hot electrons generated by AC, DC, EM, and other sources. Due to the high rate of collisions, the hot electrons

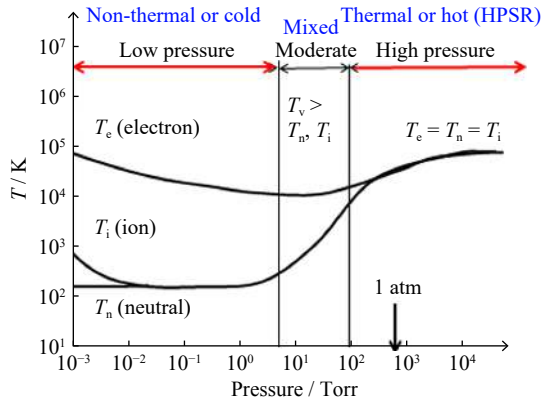

Fig. 1. Various types of hydrogen plasma and their temperatures. Reprinted by permission from Springer Nature: *Plasma Chem. Plasma Process.*, Reduction of oxide minerals by hydrogen plasma: An overview, K.C. Sabat, P. Rajput, R.K. Paramguru, B. Bhoi, and B.K. Mishra, Copyright 2013.

transfer their energy to heavy species such as H_2, H, H^+, etc. As a result, the temperatures of all these species quickly attain local thermodynamic equilibrium (LTE), i.e., all species have the same amount of energy in each degree of freedom, as shown in Fig. 1. Anything that comes into contact with thermal plasma gets heated as if it is hot gas, with the free electrons enhancing the thermal conduction. DC thermal plasmas can be divided into transferred and non-transferred arcs. In transferred arc, one of the electrodes is the workpiece, i.e., the charge or melt in metallurgical applications. In non-transferred arcs, the arc is created between two electrodes within a plasma torch, and the jet of plasma issuing from the torch is used for the metallurgical process. Typical metallurgical applications of thermal plasmas include welding, plasma spraying, plasma cutting, waste treatment, nanoparticle manufacturing, spheroidization, arc furnaces, and other metallurgical applications. The elevated temperatures, massive heat fluxes, and intense radiative emissions that define thermal plasmas are used in these applications.

3.2. Non-thermal plasmas

A cold plasma, also known as a non-thermal plasma, is a cool excited gas that can be touched even with a finger. Because the electrons have a low mass, they gain EM energy quickly and become heated. They are, however, unable to transfer their energy to heavy mass gas particles due to the low pressure. As a result, the gas remains cold. The golden example is the mercury gas inside a fluorescent tube. The free electrons in the low-pressure gas have temperatures of around 10000 K. In contrast, the gas remains near room temperature; the heavier ions and uncharged mercury atoms couple to the material of the tube, which stays cool. The electron temperature (T_e) plays a vital role in these plasmas. These low-pressure plasmas are used for various applications, including etching of semiconductors and thin-film deposition.

3.3. Mixed plasmas

The mixed plasmas combine the benefits of both thermal

and non-thermal plasmas. As illustrated in Fig. 1, they occur under moderate pressure. These plasmas are characterized by numerous temperatures, including the translational or kinetic temperatures of electrons (T_e), ions (T_i), and neutrals (T_g), and the vibrational (T_v) and rotational (T_r) excitation temperatures of molecules. They usually go in this order: $T_e > T_v > T_r \approx T_i \approx T_g$ [12–13]. Because most energy (above 70%) is stored in rotational and vibrational forms of H_2, more specifically called ro-vibrationally excited molecules (H_2^*), the vibrational temperature is the most relevant of the above temperatures. In these circumstances, T_v maintains high while T_g remains low. For example, T_v is at 4956 K while T_g is at 754 K [12], T_v in the temperature range 7600–8600 K while T_g is keeping at a low temperature range (638–962 K) [14]. There are many other cases of significant T_v, whereas T_g remains low [15–21]. When the stored energy in vibrations and rotations of H_2^* surpasses the dissociation energy of H_2 (4.52 eV) [22–24], the H_2^* molecule dissociates into H. The H atoms colliding the reduction interface diffuse into the crystal structure [25–26]. The diffused H atoms rapidly recombine, and the energy released by this recombination induces surface heating [27]. There have been several occurrences of surface heating produced by exothermic heat generated during surface recombination [28]. Interestingly, the heat of recombination of H (4.52 eV) is larger than the Fe–O bond dissociation energy (4.19 eV) [29]. As a result, the heat released by H recombination is enough to break the Fe–O bond at the reduction interface. The breaking of Fe–O being the rate-controlling step of hematite reduction [30], the surface recombination of H enhances the kinetics.

4. New extraction process by HP

Till now, H_2 might have been used for the industrial production of Fe. However, due to the imposed restrictions of thermodynamics and kinetics, H_2 has not been exploited for industrial production on a large scale. These limitations of H_2 can be eliminated by HP [1,4,6,31–40]. The thermodynamic and kinetic limitations could be overcome by the excited species present in HP, like H_2^*, H, H^+, etc. Apart from providing these advantages, HP can also be produced quickly in numerous ways such as DC, AC, radiofrequency (RF), microwave (MW), or any other electromagnetic (EM) field. Recently, by using a simple MW setup, various metals and alloys could be produced by HP, for example, Fe from Fe_2O_3 and iron ores [1,4,6,32–33,35,38], Cu from CuO [36], Co from Co_3O_4 [37], Ni from NiO [31,40], and alloys like FeCo alloy from Fe_2O_3 and Co_3O_4 mixture [35], CuNi alloy from the mixture of CuO and NiO [34], CuCo alloy from the mixture of CuO and Co_3O_4 [39], etc. In addition, several extensive reviews have been published on the extraction of different metals by various HPs [1,4]. Iron, being the most abundant metal, has a massive scope of extraction of iron by HP. Thermodynamics and kinetics are the potential pathways for extracting iron from hematite by HP. Therefore, thermodynamics and kinetics of reduction of hematite by HP have been discussed first.

4.1. Thermodynamics

The thermodynamic advantages provided by HP have been shown in the Ellingham diagram (Fig. 2). It is well-known that the standard Gibbs free energy change ($\Delta G^\ominus$) determines the exergonic and possibility of a reduction reaction. For a reduction to be possible in the standard state, $\Delta G^\ominus$ should be negative. $\Delta G^\ominus$ can be written as $\Delta G^\ominus = -RT \ln K$, where R is the universal gas constant, T is the temperature, K is the equilibrium constant ($K = 1/p_{O_2}$), and p_{O_2} is the oxygen partial pressure. Therefore, $\Delta G^\ominus$ is denoted by $\Delta G^\ominus = RT \ln p_{O_2}$. The relation between $\Delta G^\ominus$ ($= RT \ln p_{O_2}$) as a function of T is provided by the Ellingham diagram, shown in Fig. 2, which estimates how the changes in T, p_{O_2}, and the composition affect the chemical equilibrium of Fe_2O_3 and other iron oxides, thereby providing information on the relative stability and the reduction possibilities of these iron oxides. The chemical reactions of interest here are the reduction steps of Fe_2O_3 by the excited species present in HPs. As evident from Fig. 2, the H_2 line (i.e., H_2–H_2O line) lies below the line of the Fe_2O_3 for all temperatures. However, the H_2–H_2O line lays below the magnetite (Fe_3O_4) for temperatures above 900 K. H_2 should reduce Fe_2O_3 and Fe_3O_4. In practice, this is difficult to achieve due to the limitations of thermodynamics and kinetics. The H_2 reduction of Fe_2O_3 occurs in three steps, $Fe_2O_3 \rightarrow Fe_3O_4$ occurs first, followed by $Fe_3O_4 \rightarrow Fe_xO$, and finally $Fe_xO \rightarrow Fe$. The mineralogical name of Fe_xO is wustite, which is non-stoichiometry, with x ranging from 0.83 to 0.955. Assuming $x = 1$, oxygen removals in the above three steps are 11%, 22%, 66%, respect-

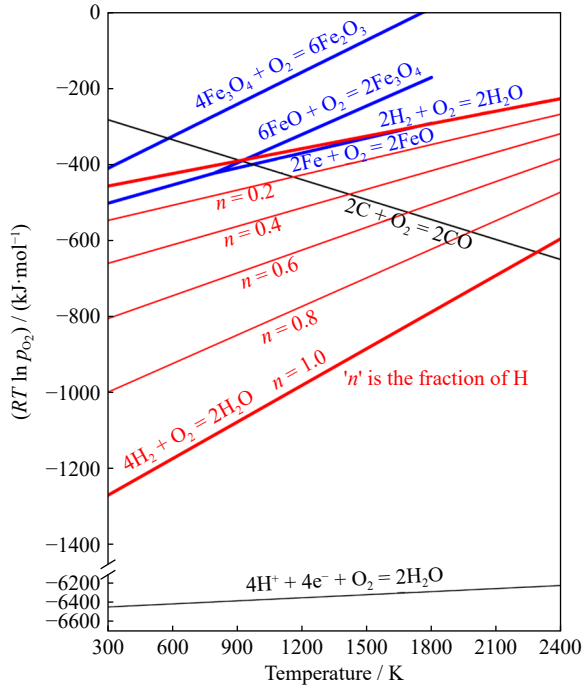

Fig. 2. Relation between $\Delta G^\ominus$ ($=RT \ln p_{O_2}$) as a function of T (Ellingham diagram) of various iron oxides, including the excited HP species. Reprinted by permission from Springer Nature: *Metall. Mater. Trans. B,* Hydrogen plasma processing of iron ore, K.C. Sabat and A.B. Murphy, Copyright 2017.

ively. For the three stages mentioned above, the following reactions can present the corresponding relevant reduction reactions:

$$3Fe_2O_3 + H_2 = 2Fe_3O_4 + H_2O,\ \Delta G_1^{\ominus} < 0,\ \text{all } T \quad (1)$$

$$Fe_3O_4 + H_2 = 3FeO + H_2O,\ \Delta G_2^{\ominus} < 0,\ \text{high } T \quad (2)$$

$$FeO + H_2 = Fe + H_2O,\ \Delta G_3^{\ominus} > 0,\ \text{all } T \quad (3)$$

The overall reaction can be written as

$$Fe_2O_3 + 3H_2 = 2Fe + 3H_2O,\ \Delta G_4^{\ominus} > 0,\ \sim \text{all } T \quad (4)$$

The estimated $\Delta G^{\ominus}$ values of the above reactions (Eqs. (1)–(4)) have already been reported elsewhere [1]. Therefore, for simplification, the numerical values of $\Delta G^{\ominus}$ have not been provided here. However, as evident from the $\Delta G^{\ominus}$ values of the above equations, the favorable thermodynamic steps in Fe_2O_3 reduction are $Fe_2O_3 \rightarrow Fe_3O_4$ and $Fe_3O_4 \rightarrow FeO$, at temperatures more than 900 K. Therefore, these first two steps can readily be carried out just by removing the kinetic restrictions. The ultimate step, $FeO \rightarrow Fe$, which involves the maximum (66%) oxygen elimination, is endothermic. For example, as estimated by Ref. [41], at 1673 K, $\Delta G_3^{\ominus} = 3.76$ kJ/mol. The K value of reduction of $Fe_2O_3 \rightarrow FeO$ is significantly positive. This step is irreversible. However, the large K value of $FeO \rightarrow Fe$ strongly favors the reverse reaction, which is visible from Fig. 2, where the $H_2 \rightarrow H_2O$ line lays above the $Fe \rightarrow FeO$ line. HP plays a significant role in the movement of the $H_2 \rightarrow H_2O$ line downwards below the $Fe \rightarrow FeO$ line, i.e., to make the conversion of $FeO \rightarrow Fe$ feasible.

When sufficient energy E ($E = hv$, where h is the planck's constant and v is the frequency of EM wave) is supplied to H_2 molecules, they get excited to generate the HP containing various excited species such as H_2^*, H, H^+, H^{2+}, etc. The energy ($E = hv$) can be provided by thermal heating or electric discharges (i.e., AC, DC, MW, RF, IF, EM, etc.).

The production of HP can be written as

$$H_2(g) + E(=hv) = HP(H_2^*/2H/2H^+/2H^{2+}, \text{etc.}) \quad \Delta G_5^{\ominus} >> 0 \quad (5)$$

The thermodynamic coupling of the above equations (Eqs. (3)–(5)), gives rise to the overall reaction for HP reduction of FeO. The following equation can represent the overall reaction:

$$FeO + HP(H_2^*/2H/2H^+/2H^{2+}, \text{etc.}) = Fe + H_2O,$$
$$\Delta G_6^{\ominus} = \Delta G_3^{\ominus} - \Delta G_5^{\ominus} < 0 \quad (6)$$

Even at low T, $\Delta G_6^{\ominus}$ becomes negative (indicating that reduction is possible), due to the excited hydrogen species present in HP. The exact estimations of the decrease in $\Delta G^{\ominus}$ due to these exciting species have already been reported elsewhere [1]. Due to this significant decrease in $\Delta G^{\ominus}$, the reduction of $Fe_2O_3 \rightarrow Fe_3O_4 \rightarrow Fe_xO \rightarrow Fe$ is feasible even at low temperatures. Therefore, HP could produce iron even at 573 K [1,35,38]. However, thermodynamics alone couldn't be the sole reason for this reduction. Thermodynamics should be used with caution because it can only be used to foresee the limitations and possibilities. This reduction at 573 K [1,35,38] is feasible due to the thermodynamic and kinetic advantages provided by H_2^*.

4.2. Kinetics of reduction by HP

With the progress of reducing Fe_2O_3 by HP, a product layer of Fe forms at the Fe_2O_3–HP interface. Suppose the process parameters are maintained such that the diffusion of the excited H_2 species present in HP through the product Fe layer is not the slowest step [30], in that case, the reduction rate could be estimated by the quality of the excited species present in the HP and their quantity (i.e., concentration) at the Fe_2O_3–HP interface. To remove the activation barrier of Fe_2O_3 reduction, there must be an interaction of the excited species present in HP and the Fe_2O_3 at the reduction interface. As reported in the literature, depending on their internal energy, the rate coefficients of reduction of Fe_2O_3 by H_2 vary several orders of magnitude. However, in the presence of HP, there is a significant increase of internal energy due to the excited species present in HP, thereby helping to easily bypass the activation barrier of the reduction. This significant lowering of activation energy results in the faster kinetics of reduction of Fe_2O_3 by HP, as compared to H_2 [1,4].

Sabat *et al.* [1,35,38] successfully demonstrated the solid-state reduction of Fe_2O_3 by H_2 and HP. By using HP, the activation energy could be decreased from 45 to 20 kJ/mol. This significant decrease in activation energy has been ascribed to the H_2^* (n = 1 level) and other excited species present in HP. It was reported that the HP constituted of 90vol% H_2, 2vol% H, and the remaining 8vol% H_2^* (n = 1 level). The HP energy was estimated as 21.5 kJ/mol for this composition. Combining this HP energy and $\Delta G^{\ominus}$ of the reactants and products, the calculated activation energy for the reduction of Fe_2O_3 is shown in Fig. 3.

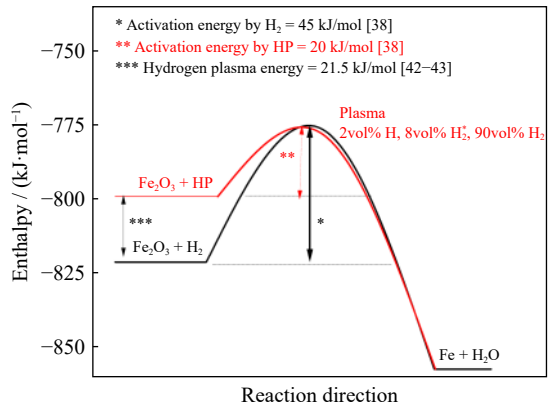

Fig. 3. Significant decline in activation energy of Fe_2O_3 reduction by replacing H_2 with HP. Reprinted by permission from Springer Nature: *Metall. Mater. Trans. B*, Hydrogen plasma processing of iron ore, K.C. Sabat and A.B. Murphy, Copyright 2017.

This significant decline of the activation energy has also been reported for Fe_2O_3–HP reduction in the liquid state. Badr [44] carried out the liquid-state reduction of Fe_2O_3 by H_2 and HP and reported a considerable decrease in activation energy due to HP. Due to this, the rate of reduction of FeO increased by almost one order magnitude. Interestingly, it has

also been observed that the reduction by HP is under chemical control. Therefore, the area of the interface plays a significant role in the reduction kinetics. Badr [44] compared the kinetics of Fe_2O_3–HP with the Fe_2O_3 reduction by CO plasma. They observed that the reduction kinetics of Fe_2O_3–HP is 3–4 times faster than Fe_2O_3 reduction by CO plasma. This is since the activation energy for the liquid-state reduction of Fe_2O_3–HP is 23 kJ/mol, only roughly 15% of the activation energy of reduction of Fe_2O_3 by CO plasma (150 kJ/mol). Therefore, HP possesses significant advantages in comparison to CO plasma.

Recently, Souza Filho *et al.* [30] concluded that the rate-controlling barriers (i.e., diffusion of oxygen species in the solid-state) in the direct reduction process do not exist in the HP process of reducing hematite, which further supports HP process of reduction is under chemical control, indicating that the reduction can be regulated by thermodynamics and kinetics.

Apart from HP's thermodynamic and kinetic advantages, the stored internal energy by the excited hydrogen species is effectively released at the reduction interface. This released energy at the interface gives local heating, which favors the reduction. Thus, no volumetric heating is involved during the Fe_2O_3–HP reduction, whereas Fe_2O_3–H_2 reduction requires volumetric heating. The volumetric heating contributes to huge heat losses from the reduction chamber. Thus, the elimination of volumetric heating in Fe_2O_3–HP reduction reduces heat loss from the reactor, thereby reducing the cost by 20% compared to the iron produced by the blast furnace process [1]. The technical and economic feasibility of the HP reduction has already been addressed in a previous publication [1]. However, the successful work that has already been on hematite reduction by various HP methods has been reviewed here.

4.3. Current state of the art

HP reduction of hematite has been carried out by (1) non-thermal or cold plasma and (2) thermal or hot plasma. The HP processing routes have been tabulated in Table 1, elaborated subsequently.

4.3.1. Non-thermal or cold HP

The reduction of Fe_2O_3 by cold HP happens in the solid-state at low temperatures, well below the melting point. Cold HP could be produced in numerous ways, as discussed earlier. The cold HP produced by MW has been used extensively by Sabat *et al.* [1,4,6,31–40]. They used a simple MW setup (similar to the microwave oven used for cooking at home), as shown in Fig. 4. The MW–HP reactor was designed to integ-

Table 1. References for different HP processing routes

Non-thermal HP reduction*	Thermal HP reduction**	
Solid-state	Liquid-state	In-flight
Sabat *et al.* [1,4, 6,31–40]	Badr [44]	Choi and Sohn [41]
Zhang *et al.* [45–46]	Gold *et al.* [47]	Gilles and Champ [63]
	MacRae [48]	Kitamura *et al.* [64]
	Kassabji and Pateyron [49]	Saito *et al.* [65]
	Nakamura *et al.* [50]	Dayal and Sadedin [66]
	Kamiya *et al.* [51]	Nikolic and Segsworth [67]
	Bäck [52]	Tylko [68–69]
	Nagasaka *et al.* [53]	Wang and Sohn [70]
	Weigel *et al.* [54]	
	Hiebler and Plaul [55]	
	Naseri Seftejani *et al.* [56–60]	
	Zarl *et al.* [61]	
	Behera *et al.* [62]	
	Souza Filho *et al.* [30]	

Note: * Solid-state, low temperature, below the melting point; ** Liquid-state, elevated temperature, above melting point.

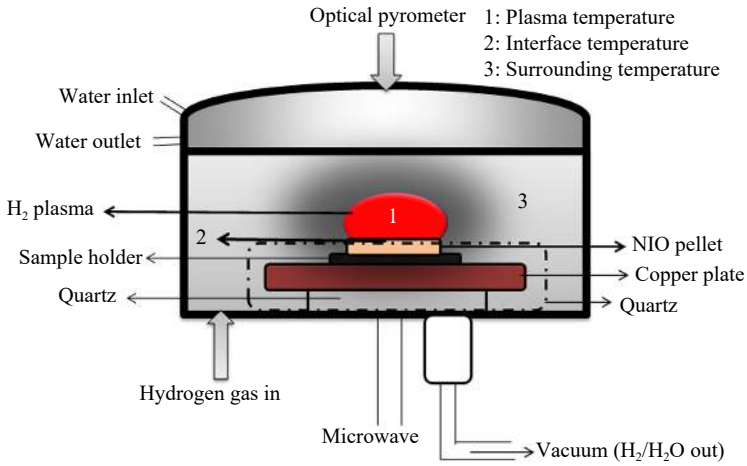

Fig. 4. Microwave HP setup used by Sabat *et al.* [1,4,6,31–40]. Reprinted by permission from Springer Nature: *Plasma Chem. Plasma Process.*, Production of nickel by cold hydrogen plasma, K.C. Sabat, Copyright 2021.

rate a power supply up to 6000 W and a microwave generator with a frequency of 2.45 GHz. HPs of high-power densities could be created by the interaction of 2.45 GHz MW with the polarity of H_2 molecules. The pellet/lump was placed on a molybdenum sample holder located at the center of the reduction chamber. HP was created in the middle, covering the sample. The governing variables of the HP were the MW power and H_2 flow rate. These parameters were kept constant and monitored throughout the tests. Also, temperature and pressure were regularly evaluated throughout the reduction studies. The reduction investigations were carried out for different intervals till reduction goes to almost 100% completion. Using this MW setup, Sabat *et al.* produced several metals such as nickel [31,40], copper [36], cobalt [37], iron [1,6,33,35,38] from the metal oxides or their ores.

Interestingly, they could also produce alloys of iron–cobalt [35], copper–nickel [34], copper–cobalt alloy [39], etc., from the reduction of combinations of these metal oxides. In these studies, Sabat *et al.* could reduce lumps/pellets of size up to 15 mm, employing MW power in the range from 600 to 1500 W and H_2 flow rate ranging from 70 to 500 sccm. Apart from MW, this notion of HP reduction of metal oxides can be exploited by generating HP by other techniques such as DC, AC, RF, or any other EM waves. These other techniques used for cold HP reduction of Fe_2O_3 have been addressed extensively in earlier publications [1,4]. The arrangement utilized by Sabat *et al.* [1,4,6,31–40] can alternatively be dubbed as mixed plasma.

4.3.2. Thermal HP reduction

In thermal HP, the reduction is carried out above the melting point of hematite. Thermal HP provides the thermodynamic and kinetic advantages, with a principle similar to using externally heated H_2 for fine hematite reduction by suspension ironmaking technology [5,71–72]. Of course, thermal HP is nothing more than an excited H_2 gas. The thermal HP combines elevated temperature, which ensures the reduction reaction's thermodynamic viability, and the kinetic advantage provided by the excited hydrogen species decreases the activation energy and makes the reduction kinetics faster. This combination facilitates iron production in a single stage with no carbon in the product.

In thermal HP processes, a thermal HP is formed from H_2 or an Ar–H_2 mixture. Like non-thermal HP, the thermal HP could also be produced in numerous ways: DC transferred arc, DC non-transferred arc, or an inductively-coupled RF discharge. The H_2 molecules present in H_2 gas receive energy through collisions with the hot electrons, heated by the electric or EM field. After acquiring energy, H_2 molecules become ro-vibrationally stimulated by a step-by-step process, dissociation, and finally ionization. The primary recombination of the dissociated and ionized species occurs at the HP–Fe_2O_3 interface. This recombination releases a huge amount of heat, which enhances the reduction of liquid Fe_2O_3, an endothermic reaction [1,4,6].

Thermal HP processes are classified into (1) liquid-state reduction and (2) in-flight reduction. The liquid-state HP reduction process is remarkably similar to direct smelting. The reduction of in-flight HP is equivalent to fluidized-bed reactors and suspension ironmaking technology [72].

(1) Liquid-state HP reduction.

Gold *et al.* [47] and MacRae [48] designed a single-stage falling film HP reactor, reported elsewhere [1]. This reactor consisted of a cylindrical vessel anode and a centrally positioned cathode. The reactor was designed on the principle of the kinetics of heterogeneous reactions, i.e., the rate of reduction of Fe_2O_3–HP is directly proportional to the Fe_2O_3–HP interfacial area. The size of the Fe_2O_3–HP interfacial area was increased by making a cylindrical vessel anode around a centrally located cathode. Furthermore, the rate of heterogeneous reduction reaction was improved by (1) increasing the interfacial area by melting fine solid particles and (2) extending the interaction duration by causing the liquid metal to flow down the anodic cylindrical walls. The HP was generated by a direct current arc discharge between the centrally located tungsten cathode and the cylindrical annular anode surrounding the cathode. The reducing gas consisting of H_2 and CH_4 in the volume ratio of 2:1 was introduced between the space between the centrally placed cathode and the surrounding cylindrical anode. The mixture was employed because the power consumed by a mixture of H_2 and CH_4 was less than the power used by H_2 or CH_4 alone. Therefore, a mixture was preferred. The raw material introduced was pulverized ore concentrate, which consisted a closely-specified grain size distribution with 45% less than 37 μm. The powder was injected downstream of the nozzle orifice tangentially to the strongly-swirling HP. The fines were melted due to the heat generated between the cathode and anode. The melted fines created a flowing film on the surface of the cylindrical anode. The reduction of fine particles took place in the flowing film, during their residence time of 1 to 60 s. The flowing film revealed several advantages during reduction: (1) It provided a large interfacial area for plasma gas and reductant, thus providing a considerable time of residence, favoring transfer of heat from the plasma gas to the reductant; (2) By making the cylindrical anode, the anode area increased, thereby reducing the chance of overheating the anode; (3) This increase in anode area protected the wear of anode, especially at the area of the arc root attachment. This decreased the erosion rate of the anode, thereby increasing the operating lifetime of the reactor; (4) Increasing the area of the thermally insulating wall increased the efficiency of the reactor.

The reactant absorbed heat from the plasma and melted at the anodic wall. While the flowing film fell down the reactor wall, the reactant got reduced in the molten state while dropping down the reactor. This reduced molten reactant was collected by a magnesia crucible, located at the bottom of the reactor. The molten slag and molten metal separated into two distinct layers, due to their density difference. These collected separate layers in the magnesia crucible were poured intermittently.

In this plasma setup, 84% thermal efficiency was ob-

tained, with electricity consumption at the rate of 2.65 kWh/kg of steel. This was achieved with the volume ratio of H_2 and CH_4 between 2:1 and 2.5:1 [27,73]. The theoretical value of the process energy requirement is 2.2 kWh/kg of Fe. To achieve this, several factors such as (1) use of finer iron ore, (2) use of an improved arc heater, and (3) improvement in reactor design and operation were taken into consideration while upscaling the reactor from 100 kW to 1 MW.

Similarly, another setup for a 1 MW falling-film reactor pilot plant to reduce iron ore has also been tried in France. Profitable results were obtained by using H_2 and natural gas, although the details of the setup and experimental results are not available [63]. However, this setup used hematite ore from Carol Lake at a 500 kg/h feed rate and a rate of reducing gas of 400 m^3/h. The molten metal was collected in the 0.6 m magnesia crucible at the rate of 320 kg/h, consisting of iron with impurities of S, P, C, Si, Cu, of 50, 10, 60, 60, and 70 ppm, respectively [74].

Despite the Bethlehem falling-film reactor's promising results, it could not find the application on an industrial scale due to the following reasons: (1) difficulty in acquiring a high-power plasma torch, (2) good working life of plasma torch, and (3) the high working voltage needed for obtaining long stable arc [75]. These successes of continuous Fe production by 1 MW plasma pilot plants showed the potential of operations with economic energy requirements. This was the remarkable turning point of thermal plasma steelmaking. Apart from steel, ferrochrome and ferrovanadium could also be produced using this 1 MW setup [73].

Nakamura *et al.* [50] melted hematite by transferred arc plasma in a water-cooled crucible. The reduced gas used for producing plasma consisted of 10% to 50% H_2 mixed with Ar. The laboratory-scale test has been reported elsewhere [1]. The degree of reduction obtained from this setup was directly proportional to the H_2 fed into the reactor. Interestingly, the H_2 utilization efficiency varied between 50% to 70%, which is much higher than the theoretical equilibrium values below 3000 K. This was ascribed to: (1) H reactivity in the HP and (2) continuous contact of HP with the molten iron oxide layer floating over the formed liquid iron. Phosphorus removal by vapor formation was significant, which depended on the $CaO/(SiO_2 + Al_2O_3)$ ratio. Better phosphorus removal occurred by Ar–H_2 plasma in comparison to Ar and Ar–N_2 plasmas.

Kamiya *et al.* [51] investigated hematite reduction by feeding with (1) batch type and (2) continuous feeding reactors. The reactors have been reported elsewhere [1]. The apparatus for batch-type feeding comprised of a DC non-transferred plasma torch with a thoriated-tungsten cathode electrode surrounded by a copper anode (water-cooled) and a transferred plasma with copper crucible anode (water-cooled). The non-transferred Ar plasma partially melted the ore. The transferred Ar plasma achieved the complete melting. After melting, the reduction was accomplished by the Ar–H_2 (7vol%) mixture. The DC power was 8.3 kW, with a gas mixture flow rate of 20 L/min for samples weighing 25 to 75 g. The reduction studies were performed for molten hematite and FeO-bearing slags. The reduction of molten hematite varied linearly with time, and the reaction rate was proportional to the partial pressure of H_2. The rate-determining step was the chemical reaction between FeO and H generated from HP via thermal dissociation. FeO-bearing slag was reduced at a slower pace than molten iron oxide, and the rate was proportional to the FeO content in the slag. The reduction of both hematite and FeO-bearing slag took place only at the melt-plasma interface formed at the cavity of the melt, which formed by the momentum of the plasma jet. In the continuous feed reactor, reduction of pre-reduced hematite was carried out. The reduction rate for continuous feeding was higher than the batch-type reactor for all H_2 flow rates.

Kamiya *et al.* [51] hypothesized the mechanism for the heterogeneous liquid–HP system formed during HP reduction of hematite. They proposed the kinetic steps as follows: (1) H_2 diffusion through the gas film from the bulk phase to the reduction interface between molten hematite and plasma gas, or the interface between the plasma and FeO-bearing slag, (2) O_2 diffusion from the molten hematite or molten FeO-bearing slag bulk to the reduction interface, through a liquid film, (3) H_2 or H adsorption at the reduction interface, (4) FeO dissociation at the reduction interface, (5) interface reduction reaction, (6) desorption of product H_2O from the reduction interface, and (7) H_2O diffusion from the reduction interface to the bulk phase through a gas film.

Hiebler and Plaul [55] proposed their liquid HP reduction as hydrogen plasma smelting reduction (HPSR), in which molten iron was produced from its ore in a laboratory-scale experimental setup. Their experimental results showed a concept of the industrial scale HPSR plant to continuously produce carbon-free iron melt from ore fines in a single stage. Their technology assessment revealed that HPSR could produce steel at a 20% reduced cost compared to the conventional routes of steelmaking. They also reported that HPSR could produce higher product quality without damaging the environment. The scale-up potential, thermodynamics, and kinetics of HPSR were examined by Badr *et al.* [76]. The details are available in Ref. [1]. The laboratory-scale experiments were carried out by Badr *et al.* [76] using an 8 kW DC transferred arc reactor, with a voltage of 110 V and a current of 70 A. Hollow graphite and lanthanated (1wt% La_2O_3) tungsten electrodes were used in his setup. The fine ores in 100 g batches were charged. Fine ores were also continuously fed through the hollow electrodes. The hollow electrodes supplied the H_2 or mixture (Ar–H_2) to the HP zone. H_2 or mixture (Ar–H_2) were supplied laterally via a ceramic lance located 20 mm from the melt surface, at a maximum flow rate of 5 L/min. For 30%, 40%, and 50% Ar–H_2 mixtures, they estimated the reduction degree, H_2 utilization degree, total H_2 utilization, and oxygen reduction rates. Badr *et al.* [76] studied the reduction of liquid hematite by H_2 and HP and reported a significant decline in activation energy due to the presence of HP. This decrease of activation energy enhanced the rate of reduction of FeO by almost one order. It

was also observed that the chemical reaction controlled the HP reduction process. Hence, the FeO–HP interfacial area played a substantial role in reduction kinetics. Badr [44] studied batch type and continuous feeding and could establish a stable arc by continuously feeding fine ores through the hollow electrode. The reduction rate also increased by 20% compared to batch loading. These advantages of continuous ore feeding opened the possibility of the scale-up process.

After the promising results for scaling up potential by Badr *et al.* [44,76], the Chair of Ferrous Metallurgy at Montanuniversitaet Leoben restarted the work on HPSR. Naseri Seftejani and Schenk [56] examined the kinetics and concluded that the reduction rate by H_2 is one or two orders of magnitude higher than those by other reductants. They also confirmed that HP is the most powerful reducing agent due to enhanced temperature, which is the most crucial factor influencing H_2 ionization and the rate of iron oxide reduction [58]. It was also reported that the highest reduction rate could be achieved when the reduction takes place at the high-temperature region of the plasma arc. Also, they confirmed the enhancement of the reduction rate by providing negative polarity to the molten pool. Furthermore, Naseri Seftejani *et al.* [59] redesigned the 8 kW DC experimental setup with new instrumentation and equipments. In this new setup, the HP was generated between the tip of the graphite electrode as a cathode and the ignition pin located in the steel crucible containing hematite as the anode. However, they experienced difficulties with the steel electrode, which caused the liquid hematite to freeze, leading to a decrease in the reduction rate and degree of reduction. Therefore, they proposed the use of refractory material for the pilot plant.

Further, they evaluated the stability of plasma arcs in the DC-transferred arc system of the HPSR by altering the gas compositions (Ar, H_2, Ar + H_2, Ar + N_2, N_2 + H_2) and process variables [61]. Using current and voltage variations, they could evaluate the stability fields for these gas compositions. They reported that the maximum reliable power input is limited by gas composition. Ar, the most stable gas, acts as a stabilizer of gas mixtures. However, with increasing Ar, the maximum transferable power gets limited. For pure H_2, they proposed a voltage range of 150–200 V and a minimum current of 100 A for maximum reliable power input. For the range of 0–40% H_2, increasing the amount of H_2 added to Ar demands an 8-fold increase in power. In addition, the stability of the arc reduces considerably with the charging of ore. Therefore, the arc stability is dependent on the charging of iron ore and its oxygen content, and the proportion of H_2 in the Ar–H_2 mixture. They also recommended that to scale up the HPSR, the relationship between arc stability and reduction rate should be explored. Keeping in mind the industrial application of the HPSR, Naseri Seftejani *et al.* [60] examined the HPSR slag generation during batch and continuous charging of iron ore with varying slag basicity. During batch charging, the degree of H_2 utilization remained high initially, which decreased with time. However, the degree of H_2 utilization remained constant during continuous charging. The highest degrees of reduction and H_2 utilization were obtained with a slag basicity of 2.3. Thus, these findings open up the possibility of further scaling up the HPSR process on the industrial scale.

On the other hand, Behera *et al.* [62] obtained the novel dimensionless parameters while exploring the HPSR of Fe_2O_3 in a 1 kg scale specially designed reactor using a water-cooled copper crucible and a plasma torch. They evaluated the hydrodynamics and degree of reduction of HPSR by using different dimensionless parameters such as the number of stoichiometric amounts of H_2 (according to reduction reaction) fed during the process, the ratio of bath height, and reactor diameter. They obtained close to 100% reduction by maintaining the specific bath height and reactor diameter ratio. These dimensionless parameters can be the most critical ones for future scaling-up procedures on an industrial scale.

Souza Filho *et al.* [30] undertook a preliminary fundamental investigation on the phase transitions and chemical evolution at the atomic scale in the HPSR study of 9 and 15 g hematite samples. They carried out the HPSR using an arc-melting furnace, where the arc (44 V and 800 A) was struck between a tungsten electrode and the sample, separated at a distance of 6 mm. The chamber gas utilized in the investigation comprised of Ar–10vol%H_2. However, the reduction was not attainable in one cycle. Therefore, to minutely examine the phase changes and chemical composition during HPSR, they subjected the samples to the interrupted specified number of cycles with exposure to HP for 1 min in each cycle. Each cycle consisted of charging of the furnace with the oxide sample and flooding of the chamber with fresh Ar–10vol%H_2 gas mixture, HPSR, followed by solidifying the sample using the water-cooled copper hearth on which HPSR was carried out, and replenishing of the furnaces chamber with fresh Ar–10vol%H_2 gas mixture for the next cycle. The partially/completely reduced samples were examined down to atomic scale, emphasizing nano-chemistry, interface structure, composition, and phase transformation kinetics.

They concluded that the hematite reduction kinetics depended on the balance between input material mass and arc power. With increasing the number of cycles, the percentage reduction increased, and the gangue components were gradually eliminated due to their vapor pressures, especially Si as SiO. Although the total elimination of Si was not possible, sulphur and phosphorous were almost eliminated, finally producing low-impurity-content iron. The reduction kinetics of the 9 g hematite specimens was sluggish during the final 25% of the reduction. By raising the weight of the hematite to 15 g, the reduction kinetics considerably increased, occurring two times faster. It appeared that the high surface area of molten pools facilitated the transfer of oxygen to the reduction interface, consequently faster reduction of 15 g sample. However, for all cases, reduction of wustite is rate controlling.

They reported that the reduction rate obtained in HPSR employing Ar–10vol%H_2 is substantially equivalent to the

rate of direct solid-state reduction of hematite using H_2 at 850–1000°C, the temperatures prevailing in shaft-furnace [77]. Unlike the direct solid-state reduction of hematite using H_2, the diffusion of oxygen species is not rate-limiting in HPSR. Also, the net energy balance of iron oxide reduction by HPSR is exothermic, quite the opposite to the direct solid-state reduction using H_2. This characteristic ensures greater efficiency in the power consumption of HPSR. However, they did not mention any anticipated power consumption. Although the study by Souza Filho *et al.* [30] has been made only on small samples, and the comparison of HPSR has been made with a solid-state reduction of hematite by H_2, their study provides a robust inference supporting that diffusion is not rate-controlling in HP reduction; instead, the reduction remains in chemical control. Their foundational study provides a new direction for the investigations on scale-up studies on the reduction of iron ores by HPSR, a carbon-neutral alternative for green iron.

After examining the outcomes of reduction in the solid and liquid state, herewith, a comparison has been made between the reduction rates of FeO in solid phase [78] and liquid phase [79–80] in Fig. 5. Fig. 5 also compares the FeO reduction using H_2 with that of reduction by HPSR (liquid–HP) [44,52,81].

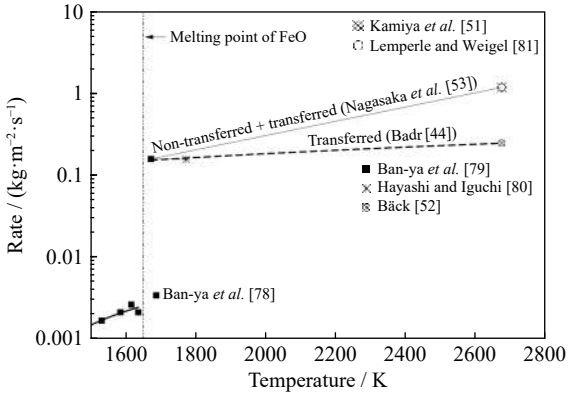

Fig. 5. Rates of reduction of FeO by H_2 and HP processes. Reprinted by permission from Springer Nature: *Metall. Mater. Trans. B,* Hydrogen plasma processing of iron ore, K.C. Sabat and A.B. Murphy, Copyright 2017.

Fig. 5 demonstrates that at the melting point, there are almost two orders of increase in reduction potential of H_2, favoring the reduction of hematite in the liquid state. However, there is only a marginal increase in the reduction rate by increasing the temperature to the plasma temperature, which lies within the same order of magnitude. However, the reduction rate increased almost one order of magnitude when transferred, and non-transferred plasmas were combined.

Surprisingly, all the above researchers [30,51,53–54,77] came to the same conclusion: the HP reduction process is chemical control. It signifies that the HP species diffuse so quickly that the diffusion barrier is broken down. As a result, if HP is employed instead of H_2, typical classic diffusion-controlled processes can be transformed into chemical-controlled processes. It is well known that chemical reactions depend on thermodynamic parameters (temperature, pressure, etc.) and kinetic parameters (activation energy, interfacial area, concentration, nature of reactants, etc.). The benefits of HP reduction have already been noted in terms of thermodynamics. The H_2^* and H recombination offer the kinetic advantage by decreasing the activation energy. Also, the concentration and nature of HP can be regulated in the solid–HP and HPSR. However, increasing the interfacial area remained a challenge in solid-HP and HPSR. The interfacial area problem can be resolved by employing fine ores, and the time of contact can be increased by applying in-flight reduction. Also, continuous feeding through a hollow electrode provides reduction enhancement of up to 20% [44]. Using non-thermal plasma increases H_2^*, lowering the activation energy, and hastening the reduction. Combining all these outcomes of the prior investigations, HP creates a new research area of in-flight reduction, which removed most of the gaps of solid-HP and HPSR.

(2) In-flight HP reduction.

Sohn and M. Olivas-Martinez [9] performed in-flight H_2 reduction of iron ore in a novel-flash reactor at a temperature higher than 1450 K and 2–3 s particle residence time. The high activation energy of 463 kJ/mol was obtained for the process, indicating significant temperature dependency. It was conclusively confirmed that iron oxide concentrate particles could be >95% reduced by H_2 in the residence time of several seconds, at 1473 K or above, typically available in the novel-flash reactor [82]. It was claimed that the energy required for the sensible heat of solid and gas feed materials and the reduction reaction of iron oxide might be supplied by a single or multiple burners or in combination with a plasma torch. Although they indicated that the plasma torch might provide sensible heat to solid and gas feed materials, they didn't mention whether HP has been employed in their flash reactor. In addition, adequate details about their flash reactor have not been documented. However, their experimental results (high activation energy, residence time, and possible use of plasma for supplying sensible heat to solid and gas materials) bring the in-flight reduction by HP into the picture. Furthermore, it has been recently established that the employment of non-thermal HP in reduction lowers the activation energy, making the reduction process under chemical reaction control, which is reliant on the emerging rate of the vibrationally-excited hydrogen molecule [1,4,6,31–40]. These facts further support the new avenue of in-flight reduction by low-temperature HP for mass production.

Despite the numerous advantages achievable by in-flight reduction, unlike HPSR, in-flight reduction has not been thoroughly researched. Nevertheless, in-flight reduction came to the limelight when Stokes achieved complete reduction by injecting hematite powder with H_2 into a helium (He) plasma [63]. The completely reduced iron powders could be collected by cold finger, 5 inches from the feed inlet. Gilles and Clump [63] carried out the in-flight reduction of iron ore by HP in a DC plasma jet reactor, reported elsewhere [1]. The setup was similar to the falling film reactor. But cathode's

outer edge consisted of tangential slots through which the plasma gas (H_2 or Ar/H_2 volume ratio of 3:1) was introduced, whereas the hematite ore fines of two size range −200+230 and −270+325 mesh size) were introduced through two opposite orifices of anode inclined at 45°. The reduced products from the in-flight reduction of oxide particles were collected on a quench plate located at 146 or 197 mm below the plasma exit nozzle. Around 70% reduction was obtained using a low hydrogen flow rate, HP gas, and finer ore size (−270+325 mesh).

Another approach called sustained shockwave plasma (shown in Fig. 6) has also been used for hematite reduction [68–69]. The cathode was placed at the centre in this plasma setup, surrounded by several anodes. First, the arc is produced between the cathode and an anode. The arc was moved from one anode to another using magnetic field coils. The magnetic field coils added pulses to the base current at 1500 Hz pulse rate, which produced compression and rarefaction pressure waves in the plasma, creating an expanded plasma of cone shape. Iron oxide particles are injected into the reactor or near the cathode, where they fall into the turbulent plasma cone. The reduction takes place in this turbulent plasma cone. The highly turbulent HP draws fine iron ores into itself, bringing them into close contact with the hottest and most energetic gas atoms over the entire volume. The goal is to "completely entrain and process enormous amounts of particle feedstock."

Kitamura *et al.* [64] demonstrated the Fe_2O_3 in-flight HP reduction by using an Ar–H_2 plasma, as shown in Fig. 7. The details have been explained elsewhere [1]. Pure Fe was obtained from reduction.

Dayal and Sadedin [66] designed a "rail reactor" for carrying out the in-flight reduction of hematite particles, as shown in Fig. 8. Hematite fines are introduced from the top of a horizontal reactor, and reduction takes place by a hori-

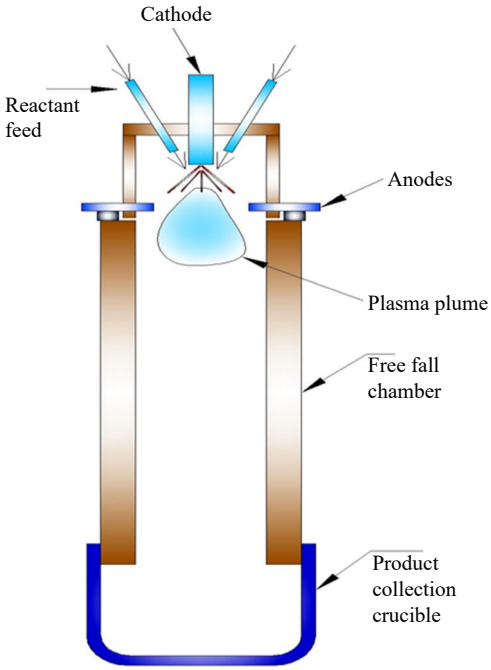

Fig. 6. Sustained shockwave plasma reactor. Reprinted by permission from Springer Nature: *Metall. Mater. Trans. B*, Hydrogen plasma processing of iron ore, K.C. Sabat and A.B. Murphy, Copyright 2017.

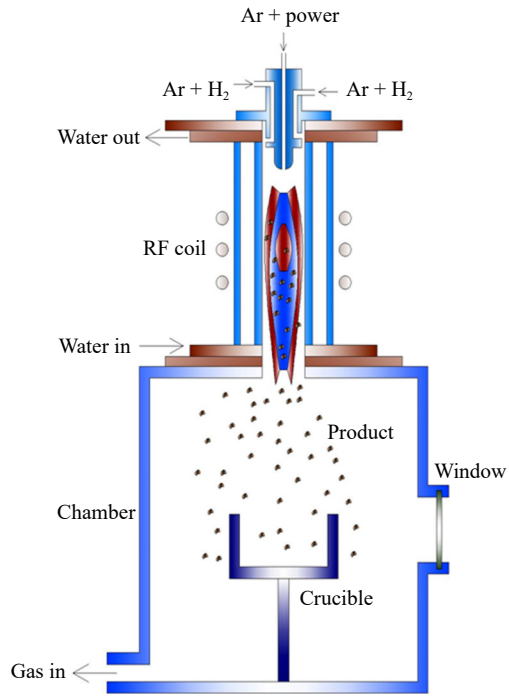

Fig. 7. In-flight HP reduction of Fe_2O_3 by using an Ar–H_2 plasma. Reprinted by permission from Springer Nature: *Metall. Mater. Trans. B*, Hydrogen plasma processing of iron ore, K.C. Sabat and A.B. Murphy, Copyright 2017.

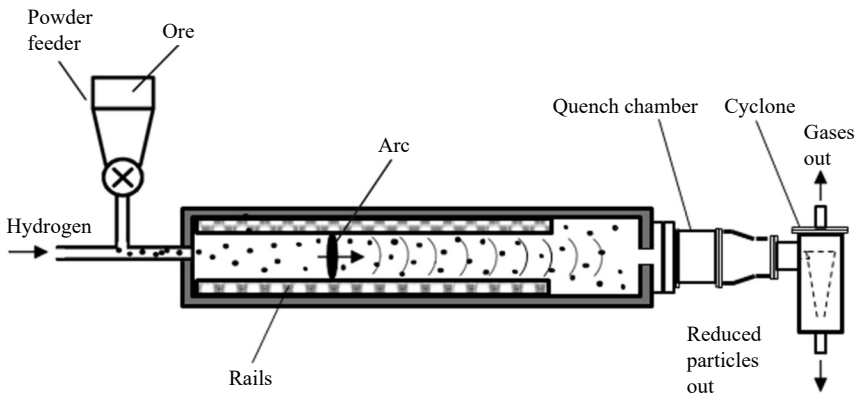

Fig. 8. Principles of design of rail reactor. Adapted from Ref. [66].

zontal transient moving arc. The rail reactor established the three factors required for successful reduction: (1) H should be available throughout the reactor's reaction volume to make the reduction faster, (2) hematite particles must remain present in HP till the completion of reduction, and (3) the temperature must be below the dissociation temperature of H_2O. The rail reactor was devised to satisfy these conditions. Results from the rail reactor showed that H could exist for sufficient time to reduce hematite; therefore, it is a promising option for the in-flight reduction of hematite.

However, the identical mechanism of the horizontal rail reactor was applied long back by Nikolic and Segsworth [67]. They called it an extended arc furnace, as shown in Fig. 9. They developed an arc furnace producing a long stable HP flame for the in-flight reduction by introducing the plasma gas through a hollow electrode. This gas produces the stable plasma required to reduce hematite descending through the plasma. The pre-heated hematite fines (38 to 295 μm) are charged from the top at a feed rate of 1 to 3 kg/h. The reduction was complete with a falling time of 200 ms. The efficiency of the reactor was higher than other plasma reactors incorporating the fluidized bed technique.

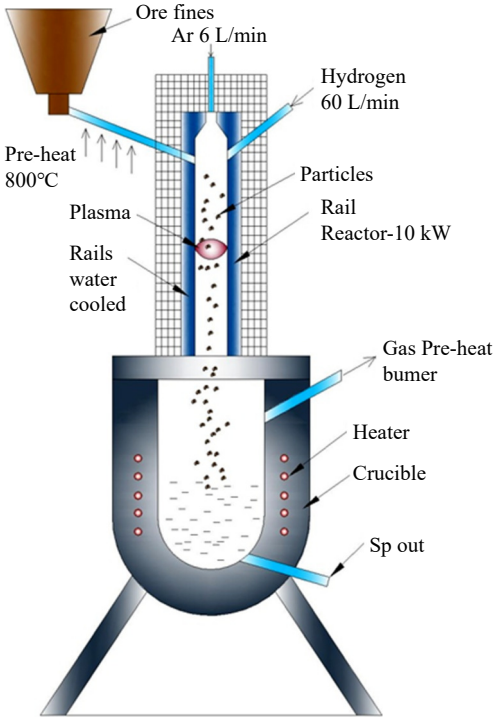

Fig. 9. Extended Arc reactor. Reprinted by permission from Springer Nature: *Metall. Mater. Trans. B*, Hydrogen plasma processing of iron ore, K.C. Sabat and A.B. Murphy, Copyright 2017.

The benefits of HP hematite reduction have been emphasized throughout the manuscript, and the drawbacks should be highlighted as well. HP reduction is influenced by several factors, the most important of which are the cost of H_2 production and HP creation. First and foremost, low-cost, non-polluting H_2 generation methods are essential for the economic sustainability of HP reduction processes. H_2 is currently produced mostly through steam methane reforming or steam extraction and the electrolysis of H_2O. The downside of steam extraction is that it releases greenhouse gases into the atmosphere, such as CO and CO_2. Electrolysis of H_2O to produce H_2 necessitates a high current through H_2O to separate hydrogen and oxygen atoms, which is energy-intensive and costly. However, electricity generated from carbon-free renewable sources such as sun, wind, and geothermal can also be used in H_2O electrolysis. Also, there are several initiatives to manufacture H_2 using semiconducting electrodes and solar radiation [1,7–8]. Furthermore, huge attempts have been made to utilize nuclear energy for the cost-effective manufacturing of massive amounts of H_2 [83–89].

The generation of HP is another issue. Thermal HP would have been preferred, but its temperatures are higher than the boiling point of Fe and the dissociation temperature of Fe oxides. Also, significant attention is essential to avoid the Fe and O reversal reaction while applying thermal HP. Another critical issue is the removal of H_2O vapor from the reduction site to shift the equilibrium towards the Fe production. In this contest, utilizing non-transferred arc HP in-flight reduction is a viable method. However, it has yet to be documented. Most of the challenges associated with thermal plasma can be overcome with non-thermal HPs. Non-thermal plasmas also contain the necessary features for successful hematite reduction, such as substantial levels of rovibrational excitation and H_2 dissociation, followed by recombination at the reduction interface. Traditional non-thermal plasmas, on the other hand, rely on a vacuum, which raises the expense. As a result, non-thermal atmospheric plasmas (i.e., divergence from LTE) are expected to accelerate the pace of reduction. In an earlier publication [1], LTE deviation has been discussed in great detail. For example, MW plasma, has T_e values 2 to 10 times larger than the temperatures of heavy species. On the other hand, microwave adds to the cost, and a counter-current solid-HP moving bed reactor employing MW has yet to be documented. A complete techno-economic feasibility analysis, on the other hand, remains a challenge!

5. Conclusions

A summary of recent progress in hydrogen plasma hematite reduction is presented. The advantages of hematite reduction by HP are as follows: (1) HP eliminates the problems associated with conventional iron production by using coal and/or H_2. In addition, HP eliminates CO_2 emissions. (2) HP can be produced in various ways, and it can be created using DC, AC, radiofrequency, microwave, or any other electromagnetic fields. (3) HP provides the thermodynamic and kinetic advantages due to the excited species, making the reduction feasible at a lower temperature. (4) There is no need for volumetric heating with HP. It merely heats the reduction interface, the requisite for reduction. Volumetric heating is eliminated, which decreases heat loss and costs. (5) The production of carbon-free iron can be accomplished in a single process, potentially eliminating the need for coke ovens, ag-

glomeration plants, blast furnaces, and oxygen steelmaking operations in future steelmaking technology. (6) The ability to accommodate finely-divided iron ore concentrates without pre-agglomeration avoids the requirement for multiple unit steps/processes in ironmaking and steelmaking. (7) The process has the potential of decreasing the cost due to the elimination of multiple operations. (8) The single-step method, which does not use carbon, offers more control than the blast furnace process. (9) In-flight reduction eliminates the majority of the shortcomings of solid-HP and HPSR. (10) Adopting in-flight reduction using non-thermal atmospheric hydrogen plasmas with high divergence from local-thermodynamic equilibrium remains a challenge!

Acknowledgement

I want to express my deep sense of gratitude to Dr. Tony Murphy of the Commonwealth Scientific and Industrial Research Organisation for serving as a friend, philosopher, and guide.

Conflict of Interest

The author declared that there is no conflicts of interests.

References

[1] K.C. Sabat and A.B. Murphy, Hydrogen plasma processing of iron ore, *Metall. Mater. Trans. B*, 48(2017), No. 3, p. 1561.

[2] E. Basson, *World Steel in Figures*, World Steel Association(2020) [2022-01-06]. https://worldsteel.org/steel-by-topic/statistics/world-steel-in-figures/

[3] A. Carpenter, *CO_2 Abatement in the Iron and Steel Industry Report CCC/193*, IEA Clean Coal Centre, London, 2012, p. 1.

[4] K.C. Sabat, P. Rajput, R.K. Paramguru, B. Bhoi, and B.K. Mishra, Reduction of oxide minerals by hydrogen plasma: An overview, *Plasma Chem. Plasma Process.*, 34(2014), No. 1, p. 1.

[5] H.Y. Sohn and Y. Mohassab, Development of a novel flash ironmaking technology with greatly reduced energy consumption and CO_2 emissions, *J. Sustainable Metall.*, 2(2016), No. 3, p. 216.

[6] K.C. Sabat, Physics and chemistry of solid state direct reduction of iron ore by hydrogen plasma, *Phys. Chem. Solid State*, 22(2021), No. 2, p. 292.

[7] X.B. Chen, S.H. Shen, L.J. Guo, and S.S. Mao, Semiconductor-based photocatalytic hydrogen generation, *Chem. Rev.*, 110(2010), No. 11, p. 6503.

[8] A. Kudo and Y. Miseki, Heterogeneous photocatalyst materials for water splitting, *Chem. Soc. Rev.*, 38(2009), No. 1, p. 253.

[9] H.Y. Sohn and M. Olivas-Martinez, Methods for calculating energy requirements for processes in which a reactant is also a fuel: Need for standardization, *JOM*, 66(2014), No. 9, p. 1557.

[10] *Plasma, Plasma, Everywhere,* National Aeronautics and Space Administration, Washington, D.C. [2022-01-05]. https://science.nasa.gov/science-news/science-at-nasa/1999/ast07sep99_1.

[11] G.H. Dieke, The molecular spectrum of hydrogen and its isotopes, *J. Mol. Spectrosc.*, 2(1958), No. 1-6, p. 494.

[12] D. Staack, B. Farouk, A. Gutsol, and A. Fridman, DC normal glow discharges in atmospheric pressure atomic and molecular gases, *Plasma Sources Sci. Technol.*, 17(2008), No. 2, p. 025013.

[13] P.J. Bruggeman, N. Sadeghi, D.C. Schram and V. Linss, Gas temperature determination from rotational lines in non-equilibrium plasmas: a review, *Plasma Sources Sci. Technol.*, 23(2014), No. 2, p. 023001.

[14] Y. Shimizu, Y. Kittaka, A. Nezu, H. Matsuura, and H. Akatsuka, Excited state distributions of hydrogen atoms in the microwave discharge hydrogen plasma and the effect of electron energy probabilistic function, *IEEE Trans. Plasma Sci.*, 43(2015), No. 5, p. 1758.

[15] V.M. Lelevkin, D.K. Otorbaev and D.C. Schram, *Physics of Non-Equilibrium Plasmas*, North-Holland Publishing Company, Amsterdam, 1992.

[16] K.R. Stalder and J.B. Jeffries, Recent results on the deposition of diamond thin films by arcjet plasmas and diagnostic measurements of the plasma-surface region, *Diam. Relat. Mater.*, 2(1993), No. 2-4, p. 443.

[17] R.G. Meulenbroeks, R.H. Engeln, M.A. Beurskens, *et al*., The argon-hydrogen expanding plasma: Model and experiments, *Plasma Sources Sci. Technol.*, 4(1995), No. 1, p. 74.

[18] F. Hummernbrum, H. Kempkens, A. Ruzicka, *et al*., Laser-induced fluorescence measurements on the C^2Sigma^+-X^2II_r transition of the CH radical produced by a microwave excited process plasma, *Plasma Sources Sci. Technol.*, 1(1992), No. 4, p. 221.

[19] J. Luque, W. Juchmann, and J.B. Jeffries, Spatial density distributions of C2, C3, and CH radicals by laser-induced fluorescence in a diamond depositing dc-arcjet, *J. Appl. Phys.*, 82(1997), No. 5, p. 2072.

[20] J. Luque, W. Juchmann, and J.B. Jeffries, Absolute concentration measurements of CH radicals in a diamond-depositing dc-arcjet reactor, *Appl. Opt.*, 36(1997), No. 15, p. 3261.

[21] V.I. Gorokhovsky, Characterization of cascade arc assisted CVD diamond coating technology: Part I. Plasma processing parameters, *Surf. Coat. Technol.*, 194(2005), No. 2-3, p. 344.

[22] W.F. Giauque, The entropy of hydrogen and the third law of thermodynamics the free energy and dissociation of hydrogen, *J. Am. Chem. Soc.*, 52(1930), No. 12, p. 4816.

[23] M.S. Vardya, Pressure dissociation and molecular hydrogen, *Mon Not R Astron Soc*, 129(1965), No. 5, p. 345.

[24] J. Meichsner, M. Schmidt, R. Schneider, and H.E. Wagner, *Nonthermal Plasma Chemistry and Physics*, 1st ed., CRC Press Inc., New York, 2012, p.121.

[25] O. Gabriel, W.E.N. van Harskamp, J.J.A. van den Dungen, D.C. Schram, and R. Engeln, Gas phase kinetics and surface interaction in a hydrogen plasma jet, [in] *The 19th International Symposium on Plasma Chemistry* (*ISPC-19*), Bochum, 2009. p. 4.

[26] Y.A. Mankelevich, M.N.R. Ashfold, and J. Ma, Plasma-chemical processes in microwave plasma-enhanced chemical vapor deposition reactors operating with C/H/Ar gas mixtures, *J. Appl. Phys.*, 104(2008), No. 11, p. 113304.

[27] A. Fridman, *Plasma Chemistry*, Cambridge University Press, New York, 2008.

[28] H. Kersten, H. Deutsch, and J. Behnke I, On the energy balance of substrate surfaces during plasma cleaning of lubricants, *Vacuum*, 48(1997), No. 2, p. 123.

[29] M.W. Chase, *NIST-JANAF Thermochemical Tables*, 4th ed., American Chemical Society, Washington, DC, 1998, p.556.

[30] I.R. Souza Filho, Y. Ma, M. Kulse, *et al*., Sustainable steel through hydrogen plasma reduction of iron ore: Process, kinetics, microstructure, chemistry, *Acta Mater.*, 213(2021), art. No. 116971.

[31] K.C. Sabat, Production of nickel by cold hydrogen plasma, *Plasma Chem. Plasma Process.*, 41(2021), No. 5, p. 1329.

[32] K.C. Sabat, Hydrogen plasma - Thermodynamics, *J. Phys.: Conf. Ser.*, 1172(2019), No. 1, art. No. 012086.

[33] K.C. Sabat, Iron production by hydrogen plasma, *J. Phys.: Conf. Ser.*, 1172(2019), No. 1, art. No. 012043.

[34] K.C. Sabat, R.K. Paramguru, and B.K. Mishra, Formation of copper–nickel alloy from their oxide mixtures through reduction by low-temperature hydrogen plasma, *Plasma Chem. Plasma Process.*, 38(2018), No. 3, p. 621.
[35] K.C. Sabat, R.K. Paramguru, and B.K. Mishra, Reduction of oxide mixtures of (Fe_2O_3+CuO) and (Fe_2O_3+Co_3O_4) by low-temperature hydrogen plasma, *Plasma Chem. Plasma Process.*, 37(2017), No. 4, p. 979.
[36] K.C. Sabat, R.K. Paramguru, and B.K. Mishra, Reduction of copper oxide by low-temperature hydrogen plasma, *Plasma Chem. Plasma Process.*, 36(2016), No. 4, p. 1111.
[37] K.C. Sabat, R.K. Paramguru, S. Pradhan, and B.K. Mishra, Reduction of cobalt oxide (Co_3O_4) by low temperature hydrogen plasma, *Plasma Chem. Plasma Process.*, 35(2015), No. 2, p. 387.
[38] P. Rajput, K.C. Sabat, R.K. Paramguru, B. Bhoi, and B.K. Mishra, Direct reduction of iron in low temperature hydrogen plasma, *Ironmaking Steelmaking*, 41(2014), No. 10, p. 721.
[39] K.C. Sabat, Formation of CuCo alloy from their oxide mixtures through reduction by low-temperature hydrogen plasma, *Plasma Chem. Plasma Process.*, 39(2019), No. 4, p. 1071.
[40] K.C. Sabat, Production of nickel by cold hydrogen plasma: role of active oxygen, *Plasma Chem. Plasma Process.*, 42(2022), No. 4, p. 833.
[41] M.E. Choi and H.Y. Sohn, Development of green suspension ironmaking technology based on hydrogen reduction of iron oxide concentrate: Rate measurements, *Ironmaking Steelmaking*, 37(2010), No. 2, p. 81.
[42] K. Hassouni, A. Gicquel, M. Capitelli, and J. Loureiro, Chemical kinetics and energy transfer in moderate pressure H_2 plasmas used in diamond MPACVD processes, *Plasma Sources Sci. Technol.*, 8(1999), No. 3, p. 494.
[43] K. Hassouni, T.A. Grotjohn, and A. Gicquel, Self-consistent microwave field and plasma discharge simulations for a moderate pressure hydrogen discharge reactor, *J. Appl. Phys.*, 86(1999), No. 1, p. 134.
[44] K. Badr, *Smelting of Iron Oxides Using Hydrogen Based Plasmas*, [Dissertation], University of Leoben, Leoben, 2007, p. 1.
[45] Y.W. Zhang, W.Z. Ding, S.Q. Guo, and K.D. Xu, Reduction of metal oxide in nonequilibrium hydrogen plasma, *Chin. J. Nonferrous Met.*, 14(2004), No. 2, p. 317.
[46] Y.W. Zhang, W.Z. Ding, X.G. Lu, S.Q. Guo, and K.D. Xu, Reduction of TiO_2 with hydrogen cold plasma in DC pulsed glow discharge, *Trans. Nonferrous Met. Soc. China*, 15(2005), No. 3, p. 594.
[47] R.G. Gold, W.R. Sandall, P.G. Cheplick, and D.R.M. Rae, Plasma reduction of iron oxide with hydrogen and natural gas at 100 kW and one megawatt, *Ironmaking Steelmaking*, 4(1977), p. 10.
[48] D.R. MacRae, *Method of Reducing Ores*, US Patent, Appl. 4002466, 1977.
[49] F. Kassabji and B. Pateyron, Technical and economical studies for metal production by plasma-steelmaking application, [in] *Proceedings of International Symposium on Plasma Chemistry 4*, Zurich, 1979, p. 236.
[50] Y. Nakamura, M. Ito, and H. Ishikawa, Reduction and dephosphorization of molten iron oxide with hydrogen-argon plasma, *Plasma Chem. Plasma Process.*, 1(1981), No. 2, p. 149.
[51] K. Kamiya, N. Kitahara, I. Morinaka, K. Sakuraya, M. Ozawa, and M. Tanaka, Reduction of molten iron oxide and FeO bearing slags by H_2–Ar plasma, *ISIJ Int.*, 24(1984), No. 1, p. 7.
[52] E. Bäck, *Schmelzreduktion von Eisenoxiden mit Argon-Wasserstoff-Plasma* [Dissertation], Montanuniversität Leoben, Leoben, 1998, p. 1.
[53] T. Nagasaka, M. Hino, and S. Ban-Ya, Interfacial kinetics of hydrogen with liquid slag containing iron oxide, *Metall. Mater. Trans. B*, 31(2000), No. 5, p. 945.
[54] A. Weigel, M. Lemperle, W. Lyhs and H. Wilhelmi, Experiments on the reduction of iron ores with an argon hydrogen plasma, [in] *Proceedings of International Symposium on Plasma Chemistry 7,* Eindhoven, 1985, p. 1.
[55] H. Hiebler and J.F. Plaul, Hydrogen plasma smelting reduction - An option for steelmaking in the future, *Metalurgija*, 43(2004), p. 155.
[56] M. Naseri Seftejani and J. Schenk, Kinetics of molten iron oxides reduction using hydrogen S cience and technology in steelmaking, *La Metall. Ital.*, 7(2018), p. 5.
[57] M. Naseri Seftejani and J. Schenk, Thermodynamic of liquid iron ore reduction by hydrogen thermal plasma, *Metals*, 8(2018), No. 12, p. 1051.
[58] M. Naseri Seftejani and J. Schenk, Kinetics of hydrogen plasma smelting reduction of iron oxides, [in] *7th International Congress on Science and Technology of Steelmaking* (ICS-2018), Venice, 2018.
[59] M. Naseri Seftejani, J. Schenk, and M.A. Zarl, Reduction of haematite using hydrogen thermal plasma, *Materials*, 12(2019), No. 10, art. No. E1608.
[60] M. Naseri Seftejani, J. Schenk, D. Spreitzer, and M. Andreas Zarl, Slag formation during reduction of iron oxide using hydrogen plasma smelting reduction, *Materials*, 13(2020), No. 4, art. No. 935.
[61] M.A. Zarl, M.A. Farkas, and J. Schenk, A study on the stability fields of arc plasma in the HPSR process, *Metals*, 10(2020), No. 10, p. 1394.
[62] P.R. Behera, B. Bhoi, R.K. Paramguru, P.S. Mukherjee, and B.K. Mishra, Hydrogen plasma smelting reduction of Fe_2O_3, *Metall. Mater. Trans. B*, 50(2019), No. 1, p. 262.
[63] H.L. Gilles and C.W. Clump, Reduction of iron ore with hydrogen in a direct current plasma jet, *Ind. Eng. Chem. Process Des. Dev.*, 9(1970), No. 2, p. 194.
[64] T. Kitamura, K. Shibata, and K. Takeda, In-flight reduction of Fe_2O_3, Cr_2O_3, TiO_2 and Al_2O_3 by Ar–H_2 and Ar–CH_4 plasma, *ISIJ Int.*, 33(1993), No. 11, p. 1150.
[65] K. Saito, Y. Morita, K. Okabe and K. Sanbongi, Reduction by Ar–H_2 Plasma, *Tetsu-To-Hagane.*, 63(1977), p. 510.
[66] A.R. Dayal and D.R. Sadedin, Application of pulsed traveling hydrogen arcs for metal oxide reduction, *Plasma Chem. Plasma Process.*, 23(2003), No. 4, p. 627.
[67] R.M. Nikolic and R.S. Segsworth, Extended arc furnace, *IEEE Trans. Ind. Appl.*, IA-13(1977), No. 1, p. 45.
[68] J.K. Tylko, *High Temperature Treatment of Materials,* US Patent, Appl. 3932171, 1976.
[69] J.K. Tylko, Expanded precessive plasmas, [in] *Proceedings of IUPAC Symposium on Plasma Chemistry* (*ISPC-1*), Kiel, 1973, p. 2.
[70] H.T. Wang and H.Y. Sohn, Hydrogen reduction kinetics of magnetite concentrate particles relevant to a novel flash ironmaking process, *Metall. Mater. Trans. B*, 44(2013), No. 1, p. 133.
[71] F. Chen, Y. Mohassab, S.Q. Zhang, and H.Y. Sohn, Kinetics of the reduction of hematite concentrate particles by carbon monoxide relevant to a novel flash ironmaking process, *Metall. Mater. Trans. B*, 46(2015), No. 4, p. 1716.
[72] M.E. Choi, *Suspension Hydrogen Reduction Of Iron Ore Concentrate* [Dissertation], The University of Utah, Utah, 2010.
[73] V. Dembovsky, *Plasma Metallurgy: The Principles*, 1st ed., Elsevier, New York, 1985, p.111.
[74] S.M.L. Hamblyn, Plasma technology and its application to extractive metallurgy, *Min. Sci Eng,* 9(1977), No. 3, p.151.
[75] M. Mihovsky, Thermal plasma application in metallurgy, *J. Univ. Chem. Technol. Metall.*, 45(2010), p. 3.
[76] K. Badr, E. Bäck and W. Krieger, Hydrogen plasma smelting reduction of iron oxide and its process up-scaling, [in] *Forum für Metallurgie und Werkstofftechnik*, Leoben, 2007, p. 23.

[77] S.H. Kim, X. Zhang, Y. Ma, *et al*., Influence of microstructure and atomic-scale chemistry on the direct reduction of iron ore with hydrogen at 700°C, *Acta Mater.*, 212(2021), p. 116933.
[78] S. Ban-ya, Y. Iguchi, and T. Nagasaka, Rate of reduction of liquid iron oxide with hydrogen, *Trans. Iron Steel Inst. Jpn.*, 23(1982), p. 197.
[79] S. Ban-ya, Y. Iguchi, and T. Nagasaka, Rate of reduction of liquid wustite with hydrogen, *Tetsu-to-Hagane*, 70(1984), No. 14, p. 1689.
[80] S. Hayashi and Y. Iguchi, Hydrogen reduction of liquid iron oxide fines in gas-conveyed systems, *ISIJ Int.*, 34(1994), No. 7, p. 555.
[81] M. Lemerle and A. Weigel, On the smelting reduction of iron ores with hydrogen-argon plasma, *Steel Res.*, 56(1985), No. 9, p. 465.
[82] S. Seetharaman, *Treatise on Process Metallurgy, Volume 3: Industrial Processes*, Elsevier, Waltham, 2014.
[83] L. Barreto, A. Makihira, and K. Riahi, The hydrogen economy in the 21st century: A sustainable development scenario, *Int. J. Hydrogen Energy*, 28(2003), No. 3, p. 267.
[84] J. Turner, Sustainable hydrogen production, *Science*, 305(2004), p. 972.
[85] G.F. Naterer, I. Dincer, and C. Zamfirescu, *Hydrogen Production from Nuclear Energy*, Springer, London, 2013.
[86] L. Walters, D. Wade, and D. Lewis, Transition to a nuclear/hydrogen energy system, *Nucl. Energy*, 42(2003), No. 1, p. 55.
[87] R.S. El-Emam, H. Ozcan, and C. Zamfirescu, Updates on promising thermochemical cycles for clean hydrogen production using nuclear energy, *J. Clean. Prod.*, 262(2020), p. 121424.
[88] C.W. Forsberg, Future hydrogen markets for large-scale hydrogen production systems, *Int. J. Hydrogen Energy*, 32(2007), No. 4, p. 431.
[89] D. Lewis, Hydrogen and its relationship with nuclear energy, *Prog. Nucl. Energy*, 50(2008), No. 2-6, p. 394.